Turbulent Prandtl number of a passively advected vector field in helical environment: Two-loop renormalization group result

E. Jurčišinová, M. Jurčišin, and P. Zalom
Institute of Experimental Physics, Slovak Academy of Sciences, Watsonova 47, 04001 Košice, Slovakia
(Received 10 February 2014; published 30 April 2014)

Using the field-theoretic renormalization group technique in the two-loop approximation, the influence of helicity (spatial parity violation) on the turbulent vector Prandtl number is investigated in the model of a passive vector field advected by the turbulent helical environment driven by the stochastic Navier-Stokes equation. It is shown that the presence of helicity in the turbulent environment can significantly decrease the value of the turbulent vector Prandtl number by up to 15% of its nonhelical value. This result is compared to the corresponding results obtained recently for the turbulent Prandtl number of a passively advected scalar quantity as well as for the turbulent magnetic Prandtl number of a weak magnetic field in the framework of the kinematic magnetohydrodynamic turbulence. It is shown that the behavior of the turbulent vector Prandtl number as function of the helicity parameter is much closer to the corresponding behavior of the turbulent Prandtl number of the scalar quantity than to the behavior of the turbulent magnetic Prandtl number.

DOI: 10.1103/PhysRevE.89.043023 PACS number(s): 47.10.ad, 47.27.ef, 47.27.tb

I. INTRODUCTION

One of the most significant characteristics of diffusion processes in fluids is provided by the ratio of the coefficient of kinematic viscosity to the diffusion coefficient of the given admixture. The resulting value are referred to as the Prandtl number of the corresponding admixture type [1–5]. At the same time, it is well known that while the microscopic structure of the fluids in the state with low values of the Reynolds number strongly influence the numerical values of various Prandtl numbers, in the regime of fully developed turbulence, i.e., in the regime with very high Reynolds number (in principle, $\mathrm{Re} \to \infty$), universal values known as the effective or turbulent Prandtl numbers are obtained [1,4,5].

On the other hand, one of the most effective techniques for theoretical investigation of various turbulent Prandtl numbers on the fundamental level of the corresponding microscopic models of fully developed turbulent systems are, without doubt, various renormalization group (RG) techniques, especially the most formal one, namely the field-theoretic (RG) technique (see, e.g., Refs. [6–8], and references cited therein). Quite recently, the field-theoretic RG technique was used for determining the turbulent Prandtl numbers in the second order of the corresponding perturbative expansion (in the two-loop approximation in the field-theoretic language) in the framework of the most important models of passive fields advected by the Navier-Stokes turbulent environments defined by the corresponding stochastic equations. Aside of their practical importance [9–23], these models also provide a suitable basis for comparative analysis regarding the influence of tensorial structures of various models on the corresponding advection-diffusion processes.

In this respect, first, in Refs. [24,25], where the turbulent Prandtl number of the passively advected scalar field was investigated in fully symmetric and isotropic turbulent environment driven by the stochastic Navier-Stokes equation, it was shown that the two-loop correction to the turbulent Prandtl number is surprisingly very small and is less than 2% of its leading one-loop value. It also means that the turbulent Prandtl number seems to be very stable under the perturbation theory. In addition, it is also worth mentioning that the calculated value of the turbulent Prandtl number is in rather good agreement with its experimentally measured values [2,3]. At the same time, another interesting result was obtained in Ref. [26], where the two-loop value of the turbulent magnetic Prandtl number of passively advected weak magnetic field in the framework of the kinematic magnetohydrodynamic (MHD) turbulence was calculated. Here, it was shown that not only the turbulent magnetic Prandtl number is perturbatively stable but also that the turbulent Prandtl number and the turbulent magnetic Prandtl number are equal to one another at the one-loop level as well as at the two-loop level of approximation.

In the end, there exists another model of a passively advected vector field, namely the so-called $\mathcal{A} = 0$ model, in which the "stretching term," which is present in the equation for the magnetic field in the kinematic MHD, is omitted (see, e.g., Ref. [27] for details), i.e., the vector model which is a complete analogy of the model of a passively advected scalar field, and which is interesting especially because the problem of anomalous scaling in the framework of the $\mathcal{A} = 0$ vector models resembles (in some important features) the problem of the anomalous scaling in genuine Navier-Stokes turbulence (see, e.g., Refs. [27–34]). In this respect, using the field-theoretic RG technique the two-loop value of the turbulent vector Prandtl number of a passively advected vector field by the Navier-Stokes velocity field was also calculated quite recently [35] with rather interesting observations and conclusions. First, it was shown that, unlike the aforementioned models of passively advected scalar and weak magnetic field, the two-loop correction to the one-loop value of the turbulent vector Prandtl number is considerably essential and forms 27% of its one-loop value. But a more interesting conclusion is that the two-loop value of the turbulent vector Prandtl number is very close to the common two-loop value of the turbulent Prandtl number of the scalar admixture and of the turbulent magnetic Prandtl number in the framework of the kinematic MHD turbulence. As it was shown in Ref. [35] the relative difference is less than 4% in respect to two-loop value of the turbulent Prandtl number of the model of the passive scalar advection. Thus, it seems that fully symmetric isotropic developed turbulent environments do not in fact feel the essential difference between the internal (tensor) structure

 ©2014 American Physical Society

of various passively advected quantities and, as a result, the properties of diffusion processes in all such turbulent systems are, at least, very similar.

However, on the other hand, as it was shown in Refs. [36,37], these conclusions are definitely not valid in the turbulent systems with violation of some symmetries. In this respect, in Ref. [37] it was shown that the presence of helicity (spatial parity violation) in the turbulent environments has a nontrivial impact on the corresponding diffusion processes of passively advected scalar and weak magnetic fields. Although the presence of helicity decreases the value of the corresponding turbulent Prandtl number in both cases, nevertheless, the decrease of the value of the turbulent Prandtl number as function of a parameter which describes the amount of helicity in the system is essentially faster than the corresponding decrease of the turbulent magnetic Prandtl number (in fact, it seems that the turbulent magnetic Prandtl number is relatively stable against helical effects). Thus, the difference between them increases up to almost 11% of the value of the scalar turbulent Prandtl number in the fully hecical case (let us note that in the nonhelical case their values are the same). However, to date no analogous results are available for the $\mathcal{A} = 0$ model of a vector admixture [35]. Therefore, it is still unknown whether the helical effects alter the turbulent vector Prandtl number in a manner resembling the relatively strong dependence of passive scalar admixtures (as could be suggested due to the close analogy of both models) or whether tensorial effects analogous to kinematic MHD take place. Resolution of this question is therefore subject of the present paper.

Thus, in the present paper the behavior of the turbulent vector Prandtl number of a vector passive admixture in the helical turbulent environment driven by the stochastic Navier-Stokes equation is investigated. Explicit dependence of the turbulent vector Prandtl number on the helicity parameter is found and it is shown that its behavior as function of the helicity parameter is very similar to the corresponding behavior of the turbulent Prandtl number of the passively advected scalar quantity. It means that in helical turbulent environments the crucial role for properties of the diffusion processes plays the presence of the "stretching term" in the model and, at the same time, it seems that the internal tensor structure of the advected field is much less important.

The paper is organized as follows. In Sec. II, the $\mathcal{A} = 0$ model of a passively advected vector field is defined and its field-theoretic formulation is given. In Sec. III, the ultraviolet (UV) renormalization of the model is briefly discussed. In Sec. IV, the two-loop turbulent vector Prandtl number is found as function of the helicity. Comparison with the corresponding results obtained in the models of the passively advected scalar field and passively advected weak magnetic field is given in Sec. V. The obtained results are then briefly reviewed and discussed in Sec. VI.

II. FIELD-THEORETIC FORMULATION OF THE MODEL

A. The $\mathcal{A} = 0$ model of passive vector advection

Thus, consider a solenoidal vector field $\mathbf{w} \equiv \mathbf{w}(x)$ ($\nabla \cdot \mathbf{w} = 0$) passively advected by the incompressible turbulent velocity field $\mathbf{v} \equiv \mathbf{v}(x)$ ($\nabla \cdot \mathbf{v} = 0$) obeying the following system of stochastic equations:

$$\partial_t \mathbf{w} = \nu_0 u_0 \triangle \mathbf{w} - (\mathbf{v} \cdot \nabla)\mathbf{w} - \partial \mathcal{Q} + \mathbf{f}^{\mathbf{w}}, \quad (1)$$

$$\partial_t \mathbf{v} = \nu_0 \triangle \mathbf{v} - (\mathbf{v} \cdot \nabla)\mathbf{v} - \partial \mathcal{P} + \mathbf{f}^{\mathbf{v}}, \quad (2)$$

where Eq. (1) represents an advection-diffusion equation for the vector field and Eq. (2) is the stochastic Navier-Stokes equation. Here, the following standard notation is used: $\partial_t \equiv \partial/\partial t$; $\partial_i \equiv \partial/\partial x_i$; $\triangle \equiv \partial^2$ is the Laplace operator; ν_0 is the viscosity coefficient; $\nu_0 u_0$ represents the diffusion coefficient of passively advected vector field, where dimensionless reciprocal "vector" Prandtl number is extracted explicitly; and $\mathcal{Q} \equiv \mathcal{Q}(x)$ and $\mathcal{P} \equiv \mathcal{P}(x)$ are the corresponding pressures.

As was already mentioned in the Introduction, the model is also known as the $\mathcal{A} = 0$ model. For completeness, let us note that this name is given as a result of the following consideration: The general form of the nonlinear part in Eq. (1) can be written as $-(\mathbf{v} \cdot \partial)\mathbf{w} + \mathcal{A}(\mathbf{w} \cdot \partial)\mathbf{v}$, where the parameter $\mathcal{A}$ in front of the "stretching term" $(\mathbf{w} \cdot \partial)\mathbf{v}$ is not fixed by Galilean symmetry and can be arbitrary [27,34]. If $\mathcal{A} = 0$, then one obtains the aforementioned "$\mathcal{A} = 0$ model" of passively advected vector impurity.

The transverse random noises $\mathbf{f}^{\mathbf{w}} \equiv \mathbf{f}^{\mathbf{w}}(x)$ and $\mathbf{f}^{\mathbf{v}} \equiv \mathbf{f}^{\mathbf{v}}(x)$ in Eqs. (1) and (2), respectively, provide sources for fluctuations of the fields to maintain the steady state of the studied dissipative turbulent system. Both random noises are assumed to be Gaussian distributions with zero average and with appropriate correlation functions. For $\mathbf{f}^{\mathbf{w}}$, the following general form of the correlator is assumed:

$$D_{ij}^{w}(x;0) \equiv \langle f_i^{w}(x) f_j^{w}(0)\rangle = \delta(t) C_{ij}(|\mathbf{x}|/L), \quad (3)$$

where L is an integral scale related to the corresponding stirring and C_{ij} is a function finite in the limit $L \to \infty$ which must decrease rapidly for $|\mathbf{x}| \gg L$. However, all other details of C_{ij} are unimportant in what follows.

On the other hand, the correlation function of $\mathbf{f}^{\mathbf{v}}$ is specified as follows:

$$D_{ij}^{v}(x;0) \equiv \langle f_i^{v}(x) f_j^{v}(0)\rangle = \delta(t) \int \frac{d^d\mathbf{k}}{(2\pi)^d} g_0 \nu_0^3 k^{4-d-2\varepsilon} R_{ij}(\mathbf{k}) e^{i\mathbf{k}\cdot\mathbf{x}}, \quad (4)$$

where d denotes the spatial dimension of the system [38], $\mathbf{k}$ is the wave vector, the exponent ε is restricted to the interval $0 < \varepsilon \leqslant 2$ with $\varepsilon = 2$ being its physical value which corresponds to the desired infrared (IR) energy pumping, and $g_0 \nu_0^3$ is a positive amplitude with explicitly extracted bare coupling constant g_0 (it plays the role of a formal small expansion parameter of the ordinary perturbation theory). It is related to the characteristic ultraviolet (UV) momentum scale Λ (or inner length $l \sim \Lambda^{-1}$) by the relation $g_0 \simeq \Lambda^{2\varepsilon}$ (see, e.g., Refs. [7,8] for details). The transverse projector $R_{ij}(\mathbf{k})$ describes the geometric properties of the random force and in the case when the spatial parity violation of the fluid is assumed it has the form of a mixture of a tensor and a pseudotensor,

$$R_{ij}(\mathbf{k}) = P_{ij}(\mathbf{k}) + H_{ij}(\mathbf{k}), \quad (5)$$

where

$$P_{ij}(\mathbf{k}) = \delta_{ij} - k_i k_j / k^2 \quad (6)$$

is the ordinary isotropic and nonhelical transverse projector and

$$H_{ij}(\mathbf{k}) = i\rho\, \epsilon_{ijl}\, k_l/|k| \tag{7}$$

controls the presence of the helicity in the flow. Here ϵ_{ijl} is the Levi-Civita's completely antisymmetric tensor of rank 3 and the real parameter $0 \leqslant |\rho| \leqslant 1$ determines the amount of helicity in the system. Setting $\rho = 0$ means that no violation of spatial parity is present in the system. On the other hand, setting $|\rho| = 1$, one obtains a system with maximal spatial parity violation. Physically, the nonzero helical part expresses the existence of nonzero correlations $\langle \mathbf{v} \cdot \mathrm{rot}\mathbf{v} \rangle$ in the turbulent environment.

In addition, note that in Eq. (4) the IR regularization is needed and is given by a lower integration bound m which corresponds to another integral scale. In what follows, we shall always suppose that $L \gg 1/m$.

B. Field-theoretic formulation of the model

According to the well-known theorem [39], the stochastic problem (1)–(4) is equivalent to the field-theoretic model of the doubled set of fields $\Phi = \{\mathbf{v},\mathbf{w},\mathbf{v}',\mathbf{w}'\}$ given by the action functional

$$\begin{aligned} S(\Phi) = {}& \frac{1}{2}\int dx_1\, dx_2\; v_i'(x_1) D^v_{ij}(x_1;x_2) v_j'(x_2) \\ &+ \frac{1}{2}\int dx_1\, dx_2\; w_i'(x_1) D^w_{ij}(x_1;x_2) w_j'(x_2) \\ &+ \int dx \{\mathbf{v}'[-\partial_t + \nu_0 \triangle]\mathbf{v} + \mathbf{w}'[-\partial_t + \nu_0 u_0 \triangle]\mathbf{w}\} \\ &- \int dx \{\mathbf{v}'(\mathbf{v}\cdot\partial)\mathbf{v} + \mathbf{w}'(\mathbf{v}\cdot\partial)\mathbf{w}\}, \end{aligned} \tag{8}$$

where $x_i = (t_i, \mathbf{x_i})$ with $i = 1,2$; D^w_{ij} and D^v_{ij} are defined by Eqs. (3) and (4), respectively; and $\mathbf{v}'$ and $\mathbf{w}'$ are auxiliary transverse fields of the same tensor nature as the corresponding fields $\mathbf{v}(x)$ and $\mathbf{w}(x)$. Additionally, all required summations over dummy indices are assumed but not explicitly indicated in Eq. (8).

The pressure terms $\partial\mathcal{Q}$ and $\partial\mathcal{P}$ in Eqs. (1) and (2) are omitted in action functional (8) due to the fact that both auxiliary vector fields $\mathbf{w}'(x)$ and $\mathbf{v}'(x)$ are also transverse, i.e., $\partial_i w_i' = 0$ as well as $\partial_i v_i' = 0$, and by using the integration by parts it is evident that they vanish. For example,

$$\int dt\, d^d\mathbf{x}\;\; v_i'\partial_i\mathcal{P} = -\int dt\, d^d\mathbf{x}\;\; \mathcal{P}\,\partial_i v_i' = 0.$$

The field-theoretic model given by the action functional in Eq. (8) allows the standard Feynman diagrammatic perturbation theory analysis of the problem. The corresponding set of bare propagators is given as follows (in frequency-momentum representation):

$$\langle w_i' w_j\rangle_0 = \langle w_i w_j'\rangle_0^* = \frac{P_{ij}(\mathbf{k})}{i\omega + \nu_0 u_0 k^2}, \tag{9}$$

$$\langle v_i' v_j\rangle_0 = \langle v_i v_j'\rangle_0^* = \frac{P_{ij}(\mathbf{k})}{i\omega + \nu_0 k^2}, \tag{10}$$

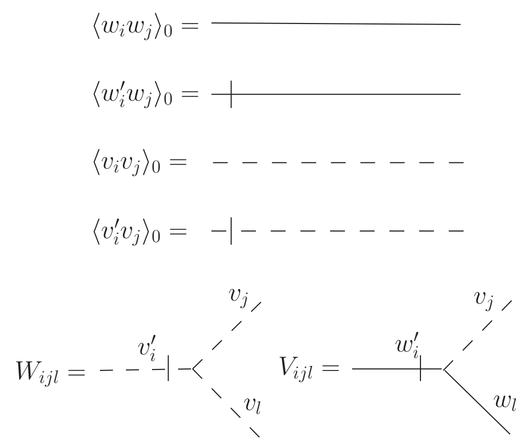

FIG. 1. Graphical representation of the bare propagators and the interaction vertices of the model.

$$\langle w_i w_j\rangle_0 = \frac{C_{ij}(\mathbf{k})}{|-i\omega + \nu_0 u_0 k^2|^2}, \tag{11}$$

$$\langle v_i v_j\rangle_0 = \frac{g_0 \nu_0^3 k^{4-d-2\varepsilon} R_{ij}(\mathbf{k})}{|-i\omega + \nu_0 k^2|^2}, \tag{12}$$

where ω is the frequency and $C_{ij}(\mathbf{k})$ is the Fourier transform of the function $C_{ij}(\mathbf{r}/L)$ in Eq. (3). Graphically, each of the propagators is represented by a corresponding line as shown in Fig. 1. Propagators involving $\mathbf{w}$ or $\mathbf{w}'$ are given by solid lines, those involving $\mathbf{v}$ or $\mathbf{v}'$ are given by dashed lines, and a slash always denotes the corresponding primed field. In addition, the model contains two triple (interaction) vertices which are given by the last line in Eq. (8), namely $-w_i'(v_j\partial_j)w_i = w_i' v_j V_{ijl} w_l$ and $-v_i' v_j \partial_j v_i = v_i' v_j W_{ijl} v_l/2$. In the frequency-momentum representation, they read $V_{ijl} = i k_j \delta_{il}$ and $W_{ijl} = i(k_l\delta_{ij} + k_j\delta_{il})$ with momentum $\mathbf{k}$ flowing into the vertices via auxiliary fields. Their graphical representation is also shown in Fig. 1.

In the end, note that formulation of the stochastic problem given by Eqs. (1)–(4) in the form of the field-theoretic model given by action functional (8) allows one to use standard RG technique to analyze the problem in the framework of which statistical averages of random quantities of the original stochastic problem are replaced with the corresponding functional averages with weight $\exp S(\Phi)$ (see, e.g., Ref. [8] for details).

III. RENORMALIZATION GROUP ANALYSIS OF THE MODEL

Typically, the RG analysis of a field-theoretic model is based on the analysis of UV divergences which, on the other hand, is given by the corresponding analysis of the canonical dimensions of the model [7,8]. Dimensional analysis of our two-scaled model shows that the coupling constant g_0 is dimensionless at $\varepsilon = 0$, i.e., the model is the so-called logarithmic at this point. Consequently, in the framework of the minimal subtraction (MS) scheme [8,40], which is always used in what follows, all possible UV divergences in the correlation functions of the model have the form of poles in ε.

Using symmetry properties of the model and the general expression for the total canonical dimension of an arbitrary

1-irreducible Green's function $\langle\Phi\cdots\Phi\rangle_{1-ir}$, which plays the role of the formal index of the UV divergence, one finds that for $d>2$ the superficial UV divergencies are present only in the 1-irreducible Green's functions $\langle v'_i v_j\rangle_{1-ir}$ and $\langle w'_i w_j\rangle_{1-ir}$. At the same time, action functional (8) has all necessary terms to remove divergences multiplicatively (see Refs. [8,40] for details). All divergencies can be removed by introducing counterterms of the form $\mathbf{v}'\Delta\mathbf{v}$ and $\mathbf{w}'\Delta\mathbf{w}$. It can be expressed explicitly in the multiplicative renormalization of the parameters g_0, u_0, and ν_0 in the form

$$\nu_0=\nu Z_\nu,\quad g_0=g\mu^{2\varepsilon}Z_g,\quad u_0=uZ_u, \tag{13}$$

where the dimensionless parameters g, u, and ν represent the renormalized counterparts of the corresponding bare ones; μ is the renormalization mass (a scale setting parameter), an artifact of the dimensional regularization; and the quantities Z_ν, Z_g, and Z_u are the corresponding renormalization constants which contain poles in ε.

Furthermore, the renormalized action functional acquires the following form:

$$\begin{aligned}S(\Phi)=&\frac{1}{2}\int dx_1\,dx_2\;v'_i(x_1)D^v_{ij}(x_1;x_2)v'_j(x_2)\\&+\frac{1}{2}\int dx_1\,dx_2\;w'_i(x_1)D^w_{ij}(x_1;x_2)w'_j(x_2)\\&+\int dx\,\mathbf{v}'[-\partial_t+\nu_0Z_1\triangle]\mathbf{v}\\&+\int dx\,\mathbf{w}'[-\partial_t+\nu_0u_0Z_2\triangle]\mathbf{w}\\&-\int dt\,d^d\mathbf{x}\,\{\mathbf{v}'(\mathbf{v}\cdot\partial)\mathbf{v}+\mathbf{w}'(\mathbf{v}\cdot\partial)\mathbf{w}\},\end{aligned} \tag{14}$$

where Z_1 and Z_2 are other renormalization constants which are related to the renormalization constants defined in Eq. (13) by the following relations:

$$Z_\nu=Z_1,\quad Z_g=Z_1^{-3},\quad Z_u=Z_2Z_1^{-1}. \tag{15}$$

Thus, the present model can be renormalized by using two independent renormalization constants, Z_1 and Z_2, and, in the framework of the MS scheme, they can be written in the following general perturbation form:

$$Z_1(g;d;\varepsilon)=1+\sum_{n=1}^{\infty}g^n\sum_{j=1}^{n}\frac{z^{(1)}_{nj}(d)}{\varepsilon^j}, \tag{16}$$

$$Z_2(g,u;d;\varepsilon)=1+\sum_{n=1}^{\infty}g^n\sum_{j=1}^{n}\frac{z^{(2)}_{nj}(u,d)}{\varepsilon^j}, \tag{17}$$

where coefficients $z^{(1)}_{nj}$ and $z^{(2)}_{nj}$ are independent of ε and follow from the requirement of UV finiteness when the 1-irreducible Green's functions $\langle v'_i v_j\rangle_{1-ir}$ and $\langle w'_i w_j\rangle_{1-ir}$ are written in terms of the renormalized parameters, i.e., they have no singularities in the limit $\varepsilon\to0$. On the other hand, the 1-irreducible Green's functions $\langle v'_i v_j\rangle_{1-ir}$ and $\langle w'_i w_j\rangle_{1-ir}$ are related to the corresponding self-energy operators $\Sigma^{v'v}$ and $\Sigma^{w'w}$, which obey the Dyson equations (the frequency-momentum representation is used)

$$\langle v'_i v_j\rangle_{1-ir}=[i\omega-\nu_0p^2+\Sigma^{v'v}(\omega,p)]P_{ij}(\mathbf{p}), \tag{18}$$

$$\langle w'_i w_j\rangle_{1-ir}=[i\omega-\nu_0u_0p^2+\Sigma^{w'w}(\omega,p)]P_{ij}(\mathbf{p}). \tag{19}$$

Consequently, Z_1 and Z_2 are found from the requirement that UV divergences do not appear in (18) and (19) after the substitution of $e_0=e\mu^{d_e}Z_e$ for $e=\{g,u,\nu\}$. This determines Z_1 and Z_2 up to the UV finite contributions. In the MS scheme, one fixes this ambiguity by prescribing renormalization constants in a general form of *1 + poles in* ε, a restriction that fully determines the coefficients $z^{(i)}_{nj}, i=1,2$ within the corresponding order of the perturbation theory.

The renormalization constant Z_1 is already known up to the second order in g, i.e., up to the two-loop approximation, in the nonhelical case [41] as well as in the helical case [42]. It means that the coefficients $z^{(1)}_{11}$, $z^{(1)}_{21}$, and $z^{(1)}_{22}$ in series (16) are already known (see Refs. [41,42] for their explicit forms). As it was shown in Refs. [42], the renormalization constant Z_1, at least up to the second-order approximation, is actually independent of the helicity parameter ρ.

On the other hand, the three-dimensional result for the nonhelical two-loop expansion of the renormalization constant Z_2 was calculated in Ref. [35], where it was used for calculation of the isotropic and nonhelical turbulent vector Prandtl number. However, its explicit general form was not shown in Ref. [35]. Therefore, for completeness, in the present paper we shall determine and show the full form of the coefficients $z^{(2)}_{11}$, $z^{(2)}_{21}$, and $z^{(2)}_{22}$ in the series (17) valid in the helical case with $\rho\neq0$ as well as in the nonhelical case with $\rho=0$.

Thus, to determine the coefficients $z^{(2)}_{11}$, $z^{(2)}_{21}$, and $z^{(2)}_{22}$ it is necessary to calculate the corresponding self-energy operator $\Sigma^{w'w}$ in the Dyson equation (19). On the other hand, up to the second-order approximation, the self-energy operator $\Sigma^{w'w}$ is given by the sum of singular parts of the corresponding set of the 1-irreducible Feynman diagrams which are shown in Fig. 2. Therefore, in two-loop approximation one can write

$$\Sigma^{w'w}=\Gamma^1+\Gamma^2=\Gamma^1+\sum_{l=1}^{8}s_l\Gamma^2_l, \tag{20}$$

where Γ^1 stands for one-loop contribution (given by single one-loop diagram); Γ^2 denotes the sum of all two-loop contributions, i.e., the sum of eight two-loop diagrams; and s_l with $l=1,\ldots,8$ are components of the vector

$$\mathbf{s}=(1,1,1,1/2,1,1,1,1), \tag{21}$$

which represents the symmetry coefficients of the corresponding two-loop diagrams Γ^2_l.

The singular part of Γ^1 has the following analytic form:

$$\Gamma^1=-\frac{S_d}{(2\pi)^d}\frac{g\nu p^2}{4\varepsilon}\left(\frac{\mu}{m}\right)^{2\varepsilon}\frac{d^2-3}{d(2+d)(u+1)}, \tag{22}$$

which is valid in nonhelical case as well as in helical case (however, only for $d=3$), i.e., the model is helicity blind at the one-loop level of approximation. Here, $S_d=2\pi^{d/2}/\Gamma(d/2)$ denotes the surface area of the d-dimensional unit sphere, $\Gamma(x)$ is the Euler's Gamma function, and m is an integral scale

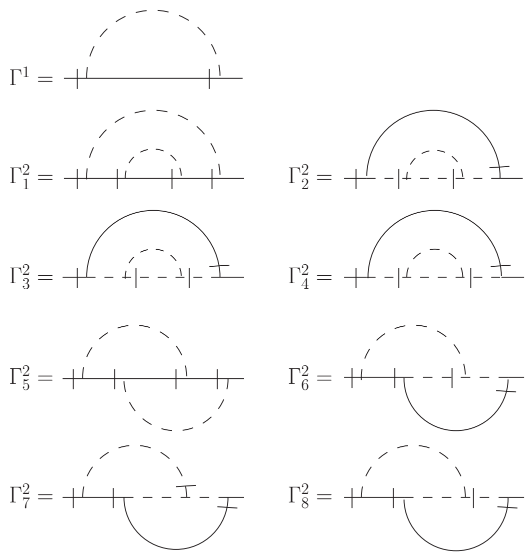

FIG. 2. The one-loop and two-loop diagrams that contribute to the self-energy operator $\Sigma^{w'w}(\omega,p)$ in Eq. (19).

related to the IR regularization. From Eq. (22) one immediately obtains

$$z_{11}^{(2)} = -\frac{S_d}{(2\pi)^d}\frac{d^2-3}{4d(2+d)u(u+1)}, \quad (23)$$

On the other hand, the result for the two-loop contribution Γ^2 to the self-energy operator $\Sigma^{w'w}$ can be written in the following integral form:

$$\Gamma^2 = \frac{g^2\nu\, p^2\, S_d}{16(2\pi)^{2d}}\left(\frac{\mu}{m}\right)^{4\varepsilon}\frac{1}{\varepsilon}\left[\frac{S_d}{2d(d+2)(1+u)\varepsilon}A + B^{(0)} + \rho^2\delta_{3d}B^{(\rho)}\right], \quad (24)$$

where

$$A = \sum_{l=1}^{8} s_l A_l \quad (25)$$

and

$$B^{(i)} = S_{d-1}\int_0^1 dx\,(1-x^2)^{(d-1)/2}\sum_{l=1}^{8} s_l B_l^{(i)}, \quad (26)$$

for $i = 0,\rho$, which represent the nonhelical ($i = 0$) and the helical ($i = \rho$) contributions. The explicit expressions for the coefficients $A_l, B_l^{(0)}$, and $B_l^{(\rho)}$ for $l = 1,\ldots,8$ are given in the Appendix. In addition, in Eq. (24) the Kronecker symbol δ_{3d} was introduced to demonstrate the fact that the helical part makes sense only for spatial dimension $d = 3$, although, for completeness, all calculations are performed in the general d-dimensional case. Note also that in Eq. (26) x is the cosine of the angle between two independent momenta $\mathbf{k}$ and $\mathbf{q}$ over which the integration is taken in two-loop diagrams, i.e., $x = \mathbf{k}.\mathbf{q}/|\mathbf{k}||\mathbf{q}|$.

Now, using the explicit expression (24) in the Dyson equation (19), the two-loop coefficients $z_{21}^{(2)}$ and $z_{22}^{(2)}$ can be immediately written as

$$z_{21}^{(2)} = \frac{S_d}{16u(2\pi)^d}\left[B^{(0)} + \rho^2\delta_{3d}B^{(\rho)}\right], \quad (27)$$

$$z_{22}^{(2)} = \frac{S_d^2}{(2\pi)^{2d}}\frac{C}{128d^2(d+2)^2u(1+u)^3}, \quad (28)$$

where $B^{(0)}$ and $B^{(\rho)}$ are given in Eq. (26) and

$$C = 36 - d^3(1+u)^2 + d(1+u)(9+5u) + 2d^4[4+u(3+u)] - 6d^2[6+u(3+u)]. \quad (29)$$

Thus, it is evident that the coefficient $z_{22}^{(2)}$ is helicity independent and the helicity enters the model only through the coefficient $z_{21}^{(2)}$ which contains the part proportional to ρ^2 [see Eq. (27)].

To proceed further it is necessary first to establish the properties of the corresponding IR scaling regime in the presence of helicity. Let us discuss it briefly.

The fact that the fields $\mathbf{v},\mathbf{v}',\mathbf{w}$, and $\mathbf{w}'$ are not renormalized in the framework of the present model leads to the following relation:

$$W^R(g,u,\nu,\mu,\ldots) = W(g_0,u_0,\nu_0,\ldots) \quad (30)$$

between the renormalized connected correlation functions $W^R = \langle\Phi\ldots\Phi\rangle^R$ and their unrenormalized counterparts $W = \langle\Phi\ldots\Phi\rangle$, where the dots stand for other arguments which are untouched by renormalization, e.g., the helicity parameter or coordinates. The difference is only in the choice of variables (renormalized or unrenormalized) and in the corresponding perturbation expansion (in g or g_0). Further, because unrenormalized correlation functions are independent of the scale-setting parameter μ, one can apply the differential operator $\mu\partial_\mu$ at fixed unrenormalized parameters on both sides of Eq. (30), which leads to the basic differential RG equation

$$[\mu\partial_\mu + \beta_g\partial_g + \beta_u\partial_u - \gamma_\nu\nu\partial_\nu]W^R(g,u,\nu,\mu,\ldots) = 0, \quad (31)$$

where the so-called RG functions (the β and γ functions) are given as follows:

$$\beta_g \equiv \mu\partial_\mu g = g(-2\varepsilon + 3\gamma_1), \quad (32)$$

$$\beta_u \equiv \mu\partial_\mu u = u(\gamma_1 - \gamma_2), \quad (33)$$

$$\gamma_i \equiv \mu\partial_\mu \ln Z_i, \quad i = 1,2, \quad (34)$$

where relations among renormalization constants (15) were used and Z_1 and Z_2 are given in (16) and (17), respectively.

Finally, the IR asymptotic scaling behavior of correlation functions of the model, i.e., the scaling behavior deep inside of the inertial interval, is driven by the IR stable fixed points of the RG equations. The coordinates (g_*,u_*) of the fixed point are given by the requirement of simultaneous vanishing of the β functions,

$$\beta_g(g_*) = 0, \quad \beta_u(g_*,u_*) = 0. \quad (35)$$

In the two-loop approximation the nontrivial fixed point with $g_* \neq 0$ and $u_* \neq 0$ has the following form:

$$g_* = g_*^{(1)}\varepsilon + g_*^{(2)}\varepsilon^2 + O(\varepsilon^3), \quad (36)$$

$$u_* = u_*^{(1)} + u_*^{(2)}\varepsilon + O(\varepsilon^2). \quad (37)$$

Here (see, e.g., Ref. [41]),

$$g_*^{(1)} = \frac{(2\pi)^d}{S_d}\frac{8(d+2)}{3(d-1)}, \tag{38}$$

$$g_*^{(2)} = g_*^{(1)}\lambda, \tag{39}$$

where λ is related to the coefficient $z_{21}^{(1)}$ in Eq. (16) as follows:

$$\lambda = \frac{2}{3}\frac{(2\pi)^{2d}}{S_d^2}\left[\frac{8(d+2)}{d-1}\right]^2 z_{21}^{(1)}. \tag{40}$$

On the other hand, the coordinate u_* of the fixed point in the two-loop approximation is given by expressions

$$u_*^{(1)} = \frac{1}{2}\left[-1+\sqrt{1+\frac{8(d^2-3)}{d(d-1)}}\right], \tag{41}$$

$$u_*^{(2)} = \frac{u_*^{(1)}\left(u_*^{(1)}+1\right)}{1+2u_*^{(1)}}\left[\lambda - \frac{128(d+2)^2}{3(d-1)^2}\mathcal{B}\left(u_*^{(1)}\right)\right], \tag{42}$$

where λ is given in Eq. (40) and the coefficient $\mathcal{B}(u_*^{(1)})$ is directly related to the coefficient $z_{21}^{(2)}$ in Eq. (27) by the following simple relation:

$$\mathcal{B}(u_*^{(1)}) = \frac{(2\pi)^{2d}}{S_d^2} z_{21}^{(2)}(u_*^{(1)}). \tag{43}$$

Let us stress once more that in the helical case ($\rho \neq 0$) the model has nontrivial sense only for spatial dimension $d = 3$, although, for completeness, we retain the d dependence of our formulas. Therefore, they can be directly used for analysis of the model in general d-dimensional space in the model without the presence of helicity.

In the end, it is also necessary to show that the fixed point is IR stable, i.e., that it really drives the IR asymptotics of the model. To this end, it is necessary to investigate the properties of the matrix of the first derivatives,

$$\Omega_{ij} = \begin{pmatrix} \partial\beta_g/\partial g & \partial\beta_g/\partial u \\ \partial\beta_u/\partial g & \partial\beta_u/\partial u \end{pmatrix}, \tag{44}$$

calculated at the fixed point (g_*,u_*). To have an IR stable fixed point the real parts of all eigenvalues of matrix (44) must be positive. However, in our case, the matrix element $\partial\beta_g/\partial u$ vanishes identically (β_g does not depend on u), therefore the eigenvalues are given directly by the diagonal elements. It can be shown by numerical analysis that both diagonal elements of the matrix (44) have positive real parts for $\varepsilon > 0$, regardless of the value of the helicity parameter ($|\rho| \leqslant 1$), i.e., the fixed point is IR attractive and its IR attractiveness is not disturbed by the presence of the spatial parity violation.

In the end, it is also worth mentioning that the form of the β functions of the present model, namely β_g and β_u in Eqs. (32) and (33), does not depend on the order of the perturbation expansion, i.e., it is exactly given by the one-loop approximation without higher-loop corrections. This fact leads to the exact values for the anomalous dimensions γ_1 and γ_2 at the IR stable fixed point (g_*,u_*) given in Eqs. (36) and (37), namely

$$\gamma_1^* = \gamma_2^* = \frac{2\varepsilon}{3}. \tag{45}$$

The very existence of the stable IR fixed point means that the correlation functions of the model exhibit scaling behavior with given critical dimensions in the IR range. However, these questions are out of scope of the present paper.

IV. THE TURBULENT VECTOR PRANDTL NUMBER IN HELICAL ENVIRONMENT

Thus, in the previous section we have performed the two-loop RG analysis of the model and all two-loop quantities needed for determining the influence of helicity on the turbulent vector Prandtl number were calculated.

Note that the two-loop RG analysis of the turbulent Prandtl number in the framework of the model of passively advected scalar quantity by the turbulent environment driven by the stochastic Navier-Stokes equation was done in Ref. [24]. There the second-order approximation RG formula for the inertial range inverse turbulent (effective) Prandtl number was derived which is independent of the renormalization scheme. The corresponding formula for the inverse turbulent vector Prandtl number was introduced recently in Ref. [35] and formally it can be written in a similar form, namely

$$u_{\rm eff} = u_*^{(1)}\Bigg(1+\varepsilon\Bigg\{\frac{1+u_*^{(1)}}{1+2u_*^{(1)}}\left[\lambda - \frac{128(d+2)^2}{3(d-1)^2}\mathcal{B}\left(u_*^{(1)}\right)\right] + \frac{(2\pi)^d}{S_d}\frac{8(d+2)}{3(d-1)}\left[a_v - a_w\left(u_*^{(1)}\right)\right]\Bigg\}\Bigg), \tag{46}$$

where $u_*^{(1)}$ is the one-loop fixed point value of the parameter u given in Eq. (41) (it also represents the one-loop value for the inverse turbulent vector Prandtl number) and the quantities λ and $\mathcal{B}(u_*^{(1)})$ are directly related to the coefficients $z_{21}^{(1)}$ and $z_{21}^{(2)}$ by the corresponding Eqs. (40) and (43), respectively. On the other hand, the quantities a_v and a_w are given by the corresponding expansions to the leading order in ε of the scaling functions of the response functions $\langle vv'\rangle$ and $\langle ww'\rangle$ for the velocity field and the advected vector field, respectively (see Ref. [24] for details). The explicit form of a_v can be found, e.g., in Ref. [24] and the explicit form of a_w in the general d-dimensional case is

$$a_w = -\frac{1}{2u(d-1)}\frac{S_{d-1}}{(2\pi)^d}\int_0^\infty dk\int_{-1}^1 dx(1-x^2)^{\frac{d-1}{2}} \times\left\{\frac{k[d(1+k^2+2kx)+k^2(x^2-2)-2kx-1]}{[k^2(1+u)+2ku+u](k^2+2kx+1)} - \theta(k-1)\frac{d-2+x^2}{(1+u)k}\right\}, \tag{47}$$

where $\theta(y)$ represents the standard Heaviside step function.

Thus, now we have all the necessary tools for determining the influence of helicity on the turbulent vector Prandtl number. As was already mentioned, the presence of helicity has sense only for spatial dimension $d = 3$. In this case, one obtains

$$u_*^{(1)} = 1, \tag{48}$$

$$\lambda = -1.0994, \tag{49}$$

$$a_v = -0.047718/(2\pi^2), \tag{50}$$

$$a_w = -0.079407/(2\pi^2), \tag{51}$$

$$\mathcal{B} = -3.9709\times10^{-3} - 0.6684\times10^{-3}\rho^2, \tag{52}$$

and, using all these facts, the final two-loop expression for the inverse turbulent vector Prandt number in helical environment has the form

$$u_{\text{eff}}(\rho) = 1 + (0.18426 + 0.11882\rho^2)\varepsilon + O(\varepsilon^2), \tag{53}$$

and for physical value $\varepsilon = 2$, one finally obtains the two-loop value of the turbulent vector Prandtl number

$$\text{Pr}_{v,t}(\rho) = u_{\text{eff}}^{-1} = \frac{1}{1.36851 + 0.23764\rho^2}. \tag{54}$$

In the nonhelical case, i.e., when $\rho = 0$, the result of Ref. [35] is recovered, i.e., $\text{Pr}_{v,t} = 0.7307$. According to Eq. (54), the turbulent vector Prandtl number decreases under the presence of the helicity monotonically down to its lowest possible value $\text{Pr}_{v,t} = 0.6226$ which is obtained for $|\rho| = 1$, i.e., in fully helical system. The difference between both extreme cases is approximately 14.8% of the nonhelical value.

Thus, we can conclude that now the behavior of the turbulent vector Prandtl number in the helical turbulent environment given by the stochastic Navier-Stokes equation is known up to the second order of the perturbative expansion. In the next section, we shall compare the obtained results to the corresponding results obtained recently for the turbulent Prandtl number of passively advected scalar field as well as for the turbulent magnetic Prandtl number of passively advected weak magnetic field in the framework of the kinematic MHD turbulence.

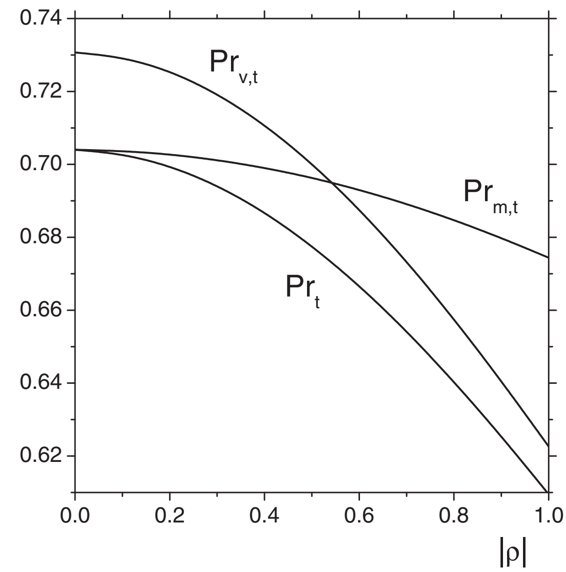

FIG. 3. The dependence of the two-loop values of various turbulent Prandtl numbers on the absolute value of the helicity parameter ρ. Here, Pr_t denotes the turbulent Prandtl number of the passive scalar admixture, $\text{Pr}_{m,t}$ stands for the turbulent magnetic Prandtl number of the kinematic MHD turbulence, and $\text{Pr}_{v,t}$ represents the turbulent vector Prandtl number of the $\mathcal{A} = 0$ model of the passively advected vector field studied in this paper.

V. TURBULENT PRANDTL NUMBERS IN HELICAL TURBULENT ENVIRONMENTS: ROLE OF TENSOR STRUCTURES IN SELECTED MODELS OF PASSIVE ADVECTION

Apart from being physically significant itself, the dependence of the turbulent vector Prandtl number on the helicity allows insights into the role of intrinsic tensor properties of advected quantities in the corresponding advection-diffusion processes. To this end, we perform comparative analysis of three different models of passively advected admixtures based on the helical effects manifested as ρ dependence of the corresponding turbulent Prandtl numbers. For the case of the $\mathcal{A} = 0$ model of a passively advected vector field, the calculation of the turbulent vector Prandtl number as function of the helicity parameter has been performed in the previous sections of this paper. The other two models involve the kinematic MHD turbulence, which describes a passive advection of the weak magnetic field, and the model of passively advected scalar field. In this respect, however, a comprehensive comparison of the corresponding turbulent Prandtl numbers in the helical environments of the last two models has been given in Ref. [37]. Let us then discuss briefly the results obtained in the present paper with respect to those obtained in Ref. [37].

In Fig. 3, the dependence of the two-loop RG values of the turbulent Prandtl number, Pr_t, of a passively advected scalar field; of the turbulent magnetic Prandtl number, $\text{Pr}_{m,t}$, of the weak magnetic field in the framework of the kinematic MHD turbulence; and the turbulent vector Prandtl number, $\text{Pr}_{v,t}$, of a passively advected vector field in the framework of the $\mathcal{A} = 0$ model on the absolute value of the helicity parameter ρ are shown simultaneously. It is evident from this figure that the behavior of the turbulent vector Prandtl number as function of the helicity is very similar to the corresponding behavior of the turbulent Prandtl number of the scalar model. In addition, quite surprisingly, their mutual difference becomes even smaller with increasing absolute value of the helicity parameter. On the other hand, the behavior of the turbulent magnetic Prandtl number as function of the helicity is quite different, namely, the difference between the turbulent magnetic Ptandtl number and the turbulent Prandtl number of the scalar model, which vanishes in the corresponding fully nonhelical turbulent environments, increases when the helicity is present and reaches the maximal value in fully helical systems. This is quite interesting behavior; therefore, let us try to understand it at the mathematical level of the tensor structure of the models.

First, note that all three models describes advection-diffusion processes of various fields by the same underlying fully developed turbulent velocity field $\mathbf{v}$ driven by the stochastic Navier-Stokes equation. However, because only passive advection is considered, the motion of the velocity field remains completely undisturbed by the presence of admixtures. It means that the evolution of the velocity field as well as all quantities related solely to the turbulent velocity field (e.g., the turbulent viscosity) are completely independent of the passive admixtures under study. In the mathematical language of the field-theoretic approach it means that all propagators, vertices, and quantities that involve only the velocity field are necessarily the same for all three studied models. Thus, it is evident that distinctive properties of all models are therefore exclusively connected to the mathematical structure of the stochastic equations which describe advected fields or, in the field-theoretic language, to the structure of propagators and interactive vertices related to the advected fields.

In this respect, the vertex V_{jkl} (see Sec. II), which involves the velocity field as well as the advected field (in the present paper it is the vector field), i.e., which describes the interaction between the turbulent velocity field and the field of a passive admixture, ends up being the most distinctive feature among the models, whereas the vertex W_{jkl}, which involves only the fields related to the velocity field itself, remains the same for all three models. As a matter of fact, two of the models, namely the $\mathcal{A}=0$ model of a passive vector admixture and the model of a passively advected scalar admixture, share the similar vertex structure even of the V vertex, namely $V_{jkl}=ip_k\delta_{jl}$ in the case of the vector model (see Sec. II) and $V_j=ip_j$ in the case of the scalar model (see, e.g., Ref. [24]). On the other hand, in the case of the corresponding model of the kinematic MHD turbulence the vertex V_{jkl} obeys additional antisymmetric property and has the form $i(p_k\delta_{jl}-p_l\delta_{jk})$ (see, e.g., Ref. [37]). Thus, because the formal mathematical difference between the $\mathcal{A}=0$ model of a passive vector admixture and the kinematic MHD turbulence is given only by the structure of the V vertex, it is evident that the antisymmetric nature of the V vertex causes a partial cancellation of the helicity contribution to the turbulent magnetic Prandtl number, i.e., the turbulent magnetic Prandtl number is much more stable against the presence of helicity than the turbulent vector Prandtl number (see Fig. 3).

On the other hand, from Fig. 3 it is immediately evident that the internal tensor structure of the advected fields has much less important impact on the diffusion processes in helical turbulent environments. This is given by the fact that the corresponding curves which describe the dependence of the turbulent Prandtl number and the turbulent vector Prandtl number on the helicity parameter have qualitatively completely the same behavior.

It is also interesting that in the nonhelical turbulent environments the situation differs substantially (at least, at the two-loop level of approximation). Here, the tensor structure of the advected field is much more important and it causes the difference between the turbulent Prandtl number of the scalar model and the turbulent vector Prandtl number of the $\mathcal{A}=0$ vector model. On the other hand, the presence of the "stretching term" in the kinematic MHD model, i.e., that the interaction vertex of the model is antisymmetric, causes an exact cancellation of the tensor effects related to the vector nature of the magnetic field and, as a result, the turbulent Prandtl number of the scalar model and the turbulent magnetic Prandtl number of the kinematic MHD turbulence have exactly the same numerical value (see Fig. 3). However, let us stress once more that this is valid only in fully nonhelical systems.

In the end, it is also worth mentioning that, due to the fact that the fixed point value of the coupling constant g^* is independent of ρ (see discussion in Sec. III as well as Refs. [42]) and, consequently, the turbulent viscosity also remains independent of the spatial parity violation, from the general definition of the corresponding turbulent Prandtl numbers (defined as ratios of the turbulent viscosity to the corresponding coefficients of turbulent diffusivity), we come to the conclusion that the corresponding turbulent diffusion coefficients increase with ρ when helicity is present in the underlying advecting environments. At the same time, all general conclusions valid for the behavior of the inverse turbulent Prandtl numbers in the helical systems are also valid for the corresponding turbulent diffusion coefficients.

VI. CONCLUSION

In this paper, we have studied the influence of helicity (spatial parity violation) on the turbulent vector Prandtl number in the framework of the model of a passive vector field advected by the turbulent helical environment driven by the stochastic Navier-Stokes equation, i.e., in the framework of the so-called $\mathcal{A}=0$ model of passively advected vector field. The explicit dependence of the turbulent vector Prandtl number on the helicity parameter ρ [see Eq. (54)] has been determined using the field-theoretic RG technique in the two-loop approximation. It is shown that the presence of helicity in the turbulent environment decreases monotonically the value of the turbulent vector Prandtl number from its nonhelical value $\mathrm{Pr}_{v,t}=0.7307$ down to the value $\mathrm{Pr}_{v,t}=0.6226$, which corresponds to fully helical system with $|\rho|=1$. The resulting change of the turbulent vector Prandtl number represents about 14.8% of its nonhelical value. The fact that the turbulent vector Prandtl number decreases as a function of the absolute value of the helicity parameter together with the fact that the turbulent viscosity is independent of helicity also means that the corresponding coefficient of turbulent diffusivity increases as function of the helicity parameter.

Additionally, we have compared the dependence of the turbulent vector Prandtl number of passively advected vector quantity on the helicity with the corresponding dependence on the helicity of the turbulent Prandtl number of passively advected scalar field as well as of the turbulent magnetic Prandtl number of passively advected weak magnetic field obtained in the framework of the kinematic MHD turbulence. It is shown that the behavior of the turbulent vector Prandtl number as function of the helicity parameter is more similar to the behavior of the turbulent Prandtl number of passively advected scalar quantity than to the corresponding behavior of the turbulent magnetic Prandtl number. The reasons for such kinds of behavior are analyzed from the point of view of the mathematical structure of the individual models. It seems that in helical turbulent environments the properties of the diffusion processes strongly depend on the form as well as on symmetry properties of the nonlinear terms in the corresponding advection-diffusion equations, which describe the interactions of advected fields with the turbulent velocity field (e.g., the presence of the "stretching term" in the kinematic MHD turbulence and its absence in the models of passively advected scalar and vector fields). At the same time, it also seems that the internal tensor structure of the advected fields is much less important in this respect.

ACKNOWLEDGMENTS

The authors gratefully acknowledge the hospitality of the Bogoliubov Laboratory of Theoretical Physics of the Joint Institute for Nuclear Research, Dubna, Russian Federation. M.J. also gratefully acknowledges the hospitality of the TH division in CERN. This work was supported by VEGA Grant No. 2/0093/13 of the Slovak Academy of Sciences and by

ITMS Project No. 26220120009, based on the supporting operational research and development program of the European Regional Development Fund.

APPENDIX

The explicit form of the coefficients $A_l, B_l^{(0)}$ and $B_l^{(\rho)}$ for $l = 1,\dots,8$ in Eqs. (25) and (26) is as follows:

$$A_1 = \frac{(d^2-3)^2}{d(d+2)(1+u)^2}, \quad A_2 = \frac{(d-1)^2(3+u)}{4(1+u)},$$

$$A_3 = \frac{(d-1)(d^2-3)}{4(d+2)}, \quad A_i = 0, \quad i = 4,\dots,8$$

$$B_1^{(0)} = \frac{(d^2-3)\left[B_{11}^{(0)}X_1 - B_{12}^{(0)}X_2\right]}{d(d-1)(d+2)x(1+u)^3},$$

$$B_2^{(0)} = -\frac{(d^2-3)}{2d(d-1)(d+2)(1+u)^2}, \times\left[B_{21}^{(0)}X_1 + B_{22}^{(0)}X_3 + B_{23}^{(0)}(X_4+X_5) + B_{24}^{(0)}X_6\right],$$

$$B_3^{(0)} = \frac{2(d^2-3)\left[B_{31}^{(0)}X_1 - B_{32}^{(0)}X_3\right]}{d(d-1)(d+2)x(1+u)},$$

$$B_4^{(0)} = -\frac{d^2-3}{4d(d-1)(d+2)x^3} \times\left[B_{41}^{(0)} + B_{42}^{(0)}X_2 + B_{43}^{(0)}X_3 - B_{44}^{(0)}X_7\right],$$

$$B_5^{(0)} = \frac{B_{51}^{(0)}X_1 - B_{52}^{(0)}X_2}{d(d-1)(d+2)(1+u)^2x},$$

$$B_6^{(0)} = \frac{2x[d^2-3-d(1-x^2)]}{(d-1)d(2+d)[1+u^2-2u(1-2x^2)](1+u)} \times\left[B_{61}^{(0)}X_1 + B_{62}^{(0)}(X_4+X_5) + B_{63}^{(0)}X_6\right],$$

$$B_7^{(0)} = \frac{1}{4d(u+1)}\left[B_{71}^{(0)} + B_{72}^{(0)}X_3 + B_{73}^{(0)}(X_4+X_5) + B_{74}^{(0)}X_2 + B_{75}^{(0)}X_6 + B_{76}^{(0)}X_7\right],$$

$$B_8^{(0)} = \frac{B_{81}^{(0)} + B_{82}^{(0)}X_1 + B_{83}^{(0)}X_2 + B_{84}^{(0)}X_3}{2(1+u)(d-1)d(2+d)x^3},$$

$$B_1^{(\rho)} = 0,$$

$$B_2^{(\rho)} = \frac{(d^2-3)(d-2)}{d(d-1)(d+2)(1+u)^2}, \times\left[B_{21}^{(\rho)}Y_1 + B_{22}^{(\rho)}Y_3 + B_{23}^{(\rho)}(Y_4+Y_5)\right],$$

$$B_3^{(\rho)} = \frac{4(d^2-3)(d-2)}{d(d-1)(d+2)(1+u)}, \times\left(2\sqrt{1-x^2}Y_1 - \frac{3-x^2}{\sqrt{4-x^2}}Y_3\right),$$

$$B_4^{(\rho)} = \frac{(d^2-3)(d-2)}{d(d-1)(d+2)(1+u)x^2}, \times\left[B_{41}^{(\rho)}Y_1 + B_{42}^{(\rho)}Y_2 + B_{43}^{(\rho)}Y_3\right],$$

$$B_5^{(\rho)} = \frac{(d-2)\left[B_{51}^{(\rho)}Y_1 + B_{52}^{(\rho)}Y_2\right]}{d(d-1)(d+2)(1+u)^2},$$

$$B_6^{(\rho)} = \frac{2(d-2)[d^2-4+x^2-d(1-x^2)]}{d(d-1)(2+d)(1+u)^2[1+u^2-2u(1-2x^2)]}, \times\left[B_{61}^{(\rho)}Y_1 + B_{62}^{(\rho)}(Y_4+Y_5)\right],$$

$$B_7^{(\rho)} = \frac{(d-2)}{2d(1+u)}, \times\left[B_{71}^{(\rho)}Y_1 + B_{72}^{(\rho)}Y_2 + B_{73}^{(\rho)}Y_3 + B_{74}^{(\rho)}(Y_4+Y_5)\right],$$

$$B_8^{(\rho)} = \frac{(d-2)\left[B_{81}^{(\rho)}Y_1 + B_{82}^{(\rho)}Y_2 + B_{83}^{(\rho)}Y_3\right]}{2d(d-1)(d+2)(1+u)x^2},$$

where

$$B_{11}^{(0)} = \frac{(1+u)(1-3x^2+2x^4)}{\sqrt{1-x^2}},$$

$$B_{12}^{(0)} = \frac{1-x^2+2u(1-dx^2)+u^2(1-3x^2+2x^4)}{\sqrt{1+2u+u^2(1-x^2)}},$$

$$B_{21}^{(0)} = 2\sqrt{1-x^2}[1+12x^2-u^3(1-4x^2)-u^2(1-16x^2) + u(1-16x^2+48x^4)]/\{x[1+u^2-2u(1-2x^2)]\},$$

$$B_{22}^{(0)} = \frac{(1+u)^2[4-(7+d)x^2+2x^4]}{(u-1)x\sqrt{4-x^2}},$$

$$B_{23}^{(0)} = 2x\{2u^3-3+2x^2+u^2(13-14x^2) + 4u(1-4x^2+2x^4) - d[1+u^2-2u(1-2x^2)]\}/ \{(1-u)\sqrt{2(1+u)-x^2}[1+u^2-2u(1-2x^2)]\},$$

$$B_{24}^{(0)} = 2\{1-2x^2-3u^2(1-2x^2)+2u[1+4x^2(1-x^2)] + d[1+u^2-2u(1-2x^2)]\}/ \{(u-1)[1+u^2-2u(1-2x^2)]\},$$

$$B_{31}^{(0)} = \frac{2(1-5x^2+4x^4)}{\sqrt{1-x^2}},$$

$$B_{32}^{(0)} = \frac{4-(7+d)x^2+2x^4}{\sqrt{4-x^2}},$$

$$B_{41}^{(0)} = \frac{2x[2+x^2(2d-5)]}{(1+u)(1-x^2)},$$

$$B_{42}^{(0)} = \frac{4\{1+u^2(1-x^2)+u[2+(d-2)x^2]\}}{(1-u)\sqrt{1+2u+u^2(1-x^2)}},$$

$$B_{43}^{(0)} = \frac{8u[4+(d-3)x^2]}{(u^2-1)\sqrt{4-x^2}},$$

$$B_{44}^{(0)} = \frac{3x^2-2+2[u-2ux^2+(d-2+u)x^4]}{(1+u)(x^2-1)^{3/2}},$$

$$B_{51}^{(0)} = (1-dx^2)\sqrt{1-x^2},$$

$$B_{52}^{(0)} = \frac{1+(5+d-2d^2)x^2-dx^4+u(1-x^2)(1-dx^2)}{\sqrt{1+2u+u^2(1-x^2)}},$$

$$B_{61}^{(0)} = -\frac{4\sqrt{1-x^2}}{1+u},$$

$$B_{62}^{(0)} = \frac{3+u-2x^2}{(1+u)\sqrt{2(1+u)-x^2}},$$

$$B_{63}^{(0)} = \frac{2x}{1-u},$$

$$B_{71}^{(0)} = \frac{2(6+u+u^3+8ux^2+4u^2x^2)}{(1+u)[1+u^2-2u(1-2x^2)]},$$

$$B_{72}^{(0)} = \frac{4(2d-x^2)}{(u-1)x\sqrt{4-x^2}},$$

$$\begin{aligned} B_{73}^{(0)} = {} & 8x\{u^4-2+2x^2-3u^3(4x^2-5) \\ & +u(12x^2-11)+u^2(8x^4-2x^2-3) \\ & -d(1+3u)[1+u^2-2u(1-2x^2)]\}/ \\ & \{(u^2-1)[1+u^2-2u(1-2x^2)]\sqrt{2(1+u)-x^2}\}, \end{aligned}$$

$$B_{74}^{(0)} = -\frac{4[1-d(1+u)-u^2(1-x^2)]}{(1+u)x\sqrt{1+2u+u^2(1-x^2)}},$$

$$\begin{aligned} B_{75}^{(0)} = {} & 8\{2x^2-1+u^3(4x^2-3)+u(4x^2-1) \\ & +u^2(5+6x^2-8x^4) \\ & +d(u-1)[1+u^2-2u(1-2x^2)]\}/ \\ & \{(1-u^2)[1+u^2-2u(1-2x^2)]^2\}, \end{aligned}$$

$$\begin{aligned} B_{76}^{(0)} = {} & (-(u-1)^5u \\ & +[u(u\{u[(u-8)(u-4)u-32]-31\}-76)-10]x^2 \\ & +8[2+u(12+u\{4+u[5+(u-4)u]\})]x^4 \\ & +16u^2(2+u^2)x^6-d[(u-1)^2+4ux^2] \\ & \times\{u-2+u^3+4[2+u(2+u)]x^2\})/ \\ & \{(1+u)x\sqrt{x^{-}1}[1+u^2-2u(1-2x^2)]^2\}, \end{aligned}$$

$$B_{81}^{(0)} = -dx(1-3x^2+2x^4),$$

$$\begin{aligned} B_{82}^{(0)} = {} & \sqrt{1-x^2}\{8x^2-3d^2x^2d(1-x^2) \\ & \times[3-2x^2+u(1-2x^2)]\}, \end{aligned}$$

$$\begin{aligned} B_{83}^{(0)} = {} & \{2d^3(1+u)x^2 \\ & +d^2x^2[-2+u(1-x^2)+3u^2(1-x^2)] \\ & +2x^2[3-u(1-x^2)-4u^2(1-x^2)] \\ & -d[1+5x^2+u^3(1-x^2)^2(1-2x^2) \\ & +u^2(3-7x^2+4x^4)+u(3+2x^2+x^4)]\}/ \\ & [(u-1)\sqrt{1+2u+u^2(1-x^2)}], \end{aligned}$$

$$\begin{aligned} B_{84}^{(0)} = {} & 2[2d^3x^2+x^2(5x^2-2)+d^2x^2(1-2x^2) \\ & +d(-4+2x^2-5x^4+x^6)]/[(1-u)\sqrt{4-x^2}], \end{aligned}$$

$$B_{21}^{(\rho)} = \frac{2\sqrt{1-x^2}\{3+u[u-1+u^2+4(3+u)x^2]\}}{1+u^2-2u(1-2x^2)},$$

$$B_{22}^{(\rho)} = \frac{(1+u)^2(3-x^2)}{(1-u)\sqrt{4-x^2}},$$

$$B_{23}^{(\rho)} = \frac{2[2-x^2+4ux^2(2-x^2)-u^2(2-5x^2)]}{(1-u)\sqrt{2(1+u)-x^2}[1+u^2-2u(1-2x^2)]},$$

$$B_{41}^{(\rho)} = \frac{2x^2-1}{(1-x^2)^{3/2}},$$

$$B_{42}^{(\rho)} = \frac{(1+u)^2}{(1-u)\sqrt{1+2u+u^2(1-x^2)}},$$

$$B_{43}^{(\rho)} = \frac{4u}{(u-1)\sqrt{4-x^2}},$$

$$B_{51}^{(\rho)} = (d+1)\sqrt{1-x^2},$$

$$B_{52}^{(\rho)} = \frac{7-2d^2-x^2+[d(1-u)-u](1-x^2)}{\sqrt{1+2u+u^2(1-x^2)}},$$

$$B_{61}^{(\rho)} = 4\sqrt{1-x^2},$$

$$B_{62}^{(\rho)} = -\frac{3+u-2x^2}{\sqrt{2(1+u)-x^2}},$$

$$B_{71}^{(\rho)} = -\frac{6+u+u^3+8ux^2+4u^2x^2}{[1+u^2-2u(1-2x^2)]\sqrt{1-x^2}},$$

$$B_{72}^{(\rho)} = \frac{2u}{\sqrt{1+2u+u^2(1-x^2)}},$$

$$B_{73}^{(\rho)} = \frac{2(1+u)}{(u-1)\sqrt{4-x^2}},$$

$$B_{74}^{(\rho)} = \frac{4(u^2-2ux^2-1)}{(u-1)[1+u^2-2u(1-2x^2)]\sqrt{2(1+u)-x^2}},$$

$$B_{81}^{(\rho)} = \frac{(d+1)(1-3x^2+2x^4)}{\sqrt{1-x^2}},$$

$$\begin{aligned} B_{82}^{(\rho)} = {} & \{(1+d)(1+u)^2-[1+d+2(d^2+d-2)u \\ & +3(1+d)u^2]x^2+2(1+d)u^2x^2\}/ \\ & [(1-u)\sqrt{1+2u+u^2(1-x^2)}], \end{aligned}$$

$$B_{83}^{(\rho)} = \frac{2[2-d^2x^2+x^4+d(2-3x^2+x^4)]}{(u-1)\sqrt{4-x^2}},$$

and

$$X_1 = \arctan\left(\frac{1+x}{\sqrt{1-x^2}}\right) - \arctan\left(\frac{1-x}{\sqrt{1-x^2}}\right),$$

$$\begin{aligned} X_2 = {} & \arctan\left[\frac{1+u(1+x)}{\sqrt{1+2u+u^2(1-x^2)}}\right] \\ & -\arctan\left[\frac{1+u(1-x)}{\sqrt{1+2u+u^2(1-x^2)}}\right], \end{aligned}$$

$$X_3 = \arctan\left(\frac{2+x}{\sqrt{4-x^2}}\right) - \arctan\left(\frac{2-x}{\sqrt{4-x^2}}\right),$$

$$X_4 = \arctan\left[\frac{2+x}{\sqrt{2(1+u)-x^2}}\right] - \arctan\left[\frac{2-x}{\sqrt{2(1+u)-x^2}}\right],$$

$$X_5 = \arctan\left[\frac{1+u+x}{\sqrt{2(1+u)-x^2}}\right] - \arctan\left[\frac{1+u-x}{\sqrt{2(1+u)-x^2}}\right],$$

$$X_6 = \ln\left(\frac{2}{1+u}\right),$$

$$X_7 = i\pi + \ln\left(\frac{1-x^2+x\sqrt{x^2-1}}{x^2-1+x\sqrt{x^2-1}}\right),$$

$$Y_1 = \pi - \arctan\left(\frac{1+x}{\sqrt{1-x^2}}\right) - \arctan\left(\frac{1-x}{\sqrt{1-x^2}}\right),$$

$$Y_2 = \pi - \arctan\left[\frac{1+u(1+x)}{\sqrt{1+2u+u^2(1-x^2)}}\right] - \arctan\left[\frac{1+u(1-x)}{\sqrt{1+2u+u^2(1-x^2)}}\right],$$

$$Y_3 = \pi - \arctan\left(\frac{2+x}{\sqrt{4-x^2}}\right) - \arctan\left(\frac{2-x}{\sqrt{4-x^2}}\right),$$

$$Y_4 = \pi - \arctan\left[\frac{2+x}{\sqrt{2(1+u)-x^2}}\right] - \arctan\left[\frac{2-x}{\sqrt{2(1+u)-x^2}}\right],$$

$$Y_5 = \pi - \arctan\left[\frac{1+u+x}{\sqrt{2(1+u)-x^2}}\right] - \arctan\left[\frac{1+u-x}{\sqrt{2(1+u)-x^2}}\right].$$

[1] A. S. Monin and A. M. Yaglom, *Statistical Fluid Mechanics* (MIT Press, Cambridge, MA, 1975), Vol. 2.

[2] L. P. Chua and R. A. Antonia, Int. J. Heat Mass Transf. **33**, 331 (1990).

[3] L. P. Chang and E. A. Cowen, J. Eng. Mech. **128**, 1082 (2002).

[4] A. Yoshizawa, S.-I. Itoh, and K. Itoh, *Plasma and Fluid Turbulence: Theory and Modelling* (Institute of Physics, Bristol, 2003).

[5] D. Biskamp, *Magnetohydrodynamic Turbulence* (Cambridge University Press, Cambridge, 2003).

[6] W. D. McComb, *The Physics of Fluid Turbulence* (Clarendon, Oxford, 1990).

[7] L. Ts. Adzhemyan, N. V. Antonov, and A. N. Vasil'ev, *The Field Theoretic Renormalization Group in Fully Developed Turbulence* (Gordon & Breach, London, 1999).

[8] A. N. Vasil'ev, *Quantum-Field Renormalization Group in the Theory of Critical Phenomena and Stochastic Dynamics* (Chapman & Hall/CRC, Boca Raton, 2004).

[9] A. M. Obukhov, Izv. Akad. Nauk. SSSR, Geogr. Geofiz. Nauk **13**, 58 (1949).

[10] K. R. Sreenivasan, Proc. R. Soc. London, Ser. A **434**, 165 (1991).

[11] C. Tong and Z. Warhaft, Phys. Fluids **6**, 2165 (1994).

[12] M. Meneguzzi and A. Pouquet, J. Fluid Mech. **205**, 297 (1989).

[13] P. D. Minnini, Phys. Plasmas **13**, 056502 (2006).

[14] Y. Ponty, P. D. Mininni, J.-F. Pinton, H. Politano, and A. Pouquet, New J. Phys. **9**, 296 (2007).

[15] A. A. Schekochihin, A. B. Iskakov, S. C. Cowley, J. C. McWilliams, M. R. E. Proctor, and T. A. Yousef, New J. Phys. **9**, 300 (2007).

[16] L. M. Malyshkin and S. Boldyrev, Phys. Rev. Lett. **105**, 215002 (2010).

[17] A. Brandenburg, Astron. Nachr. **332**, 51 (2011).

[18] T. A. Yousef, A. Brandenburg, and G. Rüdiger, Astron. Astrophys. **411**, 321 (2003).

[19] S. A. Balbus and P. Henri, Astrophys. J. **674**, 408 (2008).

[20] X. Guan and C. F. Gammie, Astrophys. J. **697**, 1901 (2009).

[21] S. Fromang, J. Papaloizou, G. Lesur, and T. Heinemann, EAS Publications **41**, 167 (2010).

[22] Nils Erland L. Haugen, A. Brandenburg, and W. Dobler, Phys. Rev. E **70**, 016308 (2004).

[23] A. Pouquet, E. Lee, M. E. Brachet, P. D. Mininni, and D. Rosenberg, Geophys. Astrophys. Fluid Dyn. **104**, 115 (2010).

[24] L. Ts. Adzhemyan, J. Honkonen, T. L. Kim, and L. Sladkoff, Phys. Rev. E **71**, 056311 (2005).

[25] E. Jurčišinová, M. Jurčišin, and R. Remecký, Phys. Rev. E **82**, 028301 (2010).

[26] E. Jurčišinová, M. Jurčišin, and R. Remecký, Phys. Rev. E **84**, 046311 (2011).

[27] N. V. Antonov, M. Hnatich, J. Honkonen, and M. Jurčišin, Phys. Rev. E **68**, 046306 (2003).

[28] I. Arad and I. Procaccia, Phys. Rev. E **63**, 056302 (2001).

[29] L. Ts. Adzhemyan, N. V. Antonov, and A. V. Runov, Phys. Rev. E **64**, 046310 (2001).

[30] L. Ts. Adzhemyan, N. V. Antonov, A. Mazzino, P. Muratore-Ginanneschi, and A. V. Runov, Europhys. Lett. **55**, 801 (2001).

[31] S. V. Novikov, Theor. Math. Phys. **136**, 936 (2003); J. Phys. A: Math. Gen. **39**, 8133 (2006).

[32] L. Ts. Adzhemyan and S. V. Novikov, Theor. Math. Phys. **146**, 393 (2006).

[33] H. Arponen, Phys. Rev. E **79**, 056303 (2009).

[34] L. Ts. Adzhemyan, N. V. Antonov, P. B. Gol'din, and M. V. Kompaniets, J. Phys. A: Math. Theor. **46**, 135002 (2013); N. V. Antonov and N. M. Gulitskiy, Theor. Math. Phys. **176**, 851 (2013).

[35] E. Jurčišinová, M. Jurčišin, and R. Remecký, Phys. Rev. E **88**, 011002(R) (2013).

[36] E. Jurčišinová, M. Jurčišin, and R. Remecký, Theor. Math. Phys. **169**, 1573 (2011); **173**, 1776 (2012).

[37] E. Jurčišinová, M. Jurčišin, R. Remecký, and P. Zalom, Phys. Rev. E **87**, 043010 (2013).

[38] Although, in the present paper we consider the turbulent environment with spatial parity violation (helicity), which is important only for spatial dimension $d = 3$, nevertheless, for completeness, we shall keep d dependence in all general formulas.

[39] P. C. Martin, E. D. Siggia, and H. A. Rose, Phys. Rev. A **8**, 423 (1973); C. De Dominicis, J. Phys. (Paris) **37**, C1-247 (1976); H. K. Janssen, Z. Phys. B **23**, 377 (1976); R. Bausch, H. K. Janssen, and H. Wagner, *ibid.* **24**, 113 (1976).

[40] J. Zinn-Justin, *Quantum Field Theory and Critical Phenomena* (Clarendon, Oxford, 1989).

[41] L. Ts. Adzhemyan, N. V. Antonov, M. V. Kompaniets, and A. N. Vasil'ev, Int. J. Mod. Phys. B **17**, 2137 (2003).

[42] E. Jurčišinová, M. Jurčišin, and R. Remecký, Phys. Rev. E **79**, 046319 (2009); **86**, 049902(E) (2012).